

TALIF measurements of atomic oxygen density in L2K plasma wind tunnel

Giuseppe Ceglia^{1,*}, Antonio Del Vecchio¹, Uwe Koch², Ali Guelhan²

1: Dept. of Diagnostic Methodologies and Measurement Techniques, CIRA Italian Center for Aerospace Research, Italy

2: Dept. of Supersonic and Hypersonic Technologies, DLR German Aerospace Center, Germany

* g.cegla@cira.it

Keywords: Two-photon LIF, Atomic oxygen, arcjet plasma flow

ABSTRACT

Absolute atomic oxygen concentration measurements using two-photon absorption laser induced fluorescence experimental technique have been carried out in high-enthalpy plasma flow. The measurements have been conducted in L2K hypersonic wind tunnel at DLR. The test campaign is performed at 600 A of arc current in air with a mass flow rate of 36 g/s and a stagnation pressure of 10^5 Pa. The averaged total enthalpy is ~ 8.4 MJ/kg and the temperature is assumed to be equal to 4218 K. The investigation has been conducted in the freestream and into the shock layer, i.e., 5 mm upstream from the model surface. The estimation of the atomic oxygen concentration is performed by using relative fluorescence signals considering xenon $6p'[3/2]_2$ transition as reference gas. The effect of the quenching for the atomic oxygen determines a reduction of the lifetimes τ , i.e., 28.8 ns in the freestream and 11.4 ns into the shock layer. The estimation of the atomic oxygen concentration is performed by using relative fluorescence signals considering xenon as reference gas. The number density is equal to $\sim 3.33 \times 10^{23}$ m⁻³ in the freestream and $\sim 15.6 \times 10^{23}$ m⁻³ into the shock layer.

1. Introduction

Space vehicles re-entering in a planetary atmosphere undergo severe environment flight conditions due to aero-thermodynamic loads impinging on the exposed surfaces. Depending on the flight altitude and Mach number, the flow around the vehicle is characterized by the presence of dissociation and ionization phenomena due to the conversion of kinetic energy into thermal energy (Anderson 1989). The environment across the shock waves results in a chemically reactive flow interacting with the heat shield of the spacecraft. Thus, the understandings of the physical and chemical processes arising during the re-entry phase are extremely important for the design of the thermal protection materials of a reusable spacecraft. Ground tests in arc-jet facilities allow for the qualification of the thermal protection materials by reproducing hypersonic high enthalpy flow fields. Computational fluid dynamics and experimental techniques are used to improve the understanding of these complex phenomena (Candler et al. 2002). In particular, non-intrusive diagnostic techniques for the characterization of the hypersonic flows are strongly required in order to perform a detailed description of their

thermodynamic state (Sharma and Park 1990). For this purpose, laser induced fluorescence (LIF) has proven to be a powerful spectroscopic non-intrusive technique to probe high enthalpy flows (Sharma et al. 1996). The main advantages of LIF technique lie in its high sensitivity and selective analysis of the chemical species. Indeed, quantities related to thermochemical properties of the freestream, i.e. species concentration, temperature, velocity and pressure reveal new insight on non-equilibrium condition. However, the large number of experimental parameters, such as laser source, detector system, optical setup, and theoretical data reduction requires a full and precise optimization (Bamford et al. 1995). LIF is the process of emission from an excited electric state of a species populated upon absorption of laser light radiation (Tropea et al. 2007). After a certain lifetime τ , this excited species can relax into a lower state by emitting fluorescence radiation. The intensity of the fluorescence can be associated with the number density (Goehlich et al 1998), translational temperature and pressure (Tropea et al. 2007, Del Vecchio et al. 2000).

As introduced before, in high enthalpy flows the presence of the atomic radicals influences the design of the thermal protection materials. Indeed among different ones, the atomic oxygen causes more interest than others because of its highly chemically reactive behaviour. Experimental investigations devoted to find out the basic understanding of the thermodynamic processes involving atomic oxygen are required. Because of the large energy difference between the ground state and the excited states of the oxygen, i.e. the first excited level of the oxygen is at 130.2 nm, two-photon absorption process is chosen, avoiding the use of lasers operating in range of vacuum ultraviolet (VUV) radiation. Indeed, this compromises the transmission of the VUV laser radiation through media at such elevated pressure, complicating the experimental setup (Niemi et al. 2001). Two-photon absorption LIF (TALIF) method circumvents this problem to excite with two photons the atomic oxygen ground state (Goehlich et al. 1998). The working principle of the TALIF is based on the simultaneously absorption of two photons by an atom in ground electronic state if their combined energies correspond to the gap between the ground and the excited state and if they arrive within the atom volume and within the lifetime of its excited state (Niemi et al. 2001).

In order to provide quantitative measurements of the concentration of atomic oxygen, calibration procedure for TALIF spectroscopy technique is required. The calibration procedure consists commonly of comparative measurements by using flow-tube reactors generator or a noble gas as reference (Goehlich et al. 1998). Because of the difficulties to provide controlled amount of species concentration from flow-tube reactor by titration, the calibration with a noble gas is technically a simple alternative. As reported by Niemi et al. (2001), xenon ($6p'[3/2]_2$ transition) satisfies the requirements of reference gas, i.e. condition of excitation and detection as similar as possible in terms of spectral behaviour. The two-photon excitation schemes of the atomic oxygen

and xenon are depicted in Fig. 1. In addition since the method is based on the absorption of two photons by the probed species, quadratic dependence of the fluorescence signal with respect to the intensity of the laser energy has to be verified in order to prevent saturation or ionization processes that can compromise the quantitative comparison. In the case of excitation with low laser intensity (order of magnitude of few μJ), depletion of the ground state species and photoionization effects can be neglected. By applying the rate equation model that describes the population kinetics (Niemi et al. 2001), the fluorescence signal S is given as:

$$S = D \frac{A_{21}}{A_{21} + Q_{21}} \frac{E^2}{(h\omega)^2} \sigma_{\omega}^{(2)} n_{gr} \quad (1)$$

Where A_{21} is the radiative decay, Q_{21} the quenching rate, E the laser energy, $h\omega$ the excitation energy, $\sigma_{\omega}^{(2)}$ the absorption cross section, n_{gr} the ground state number density and D takes into account the experimental aspects, that are, view angle, transmission of the spectral bandwidth filter along with the quantum efficiency of the detector. The fluorescence quantum yield $A_{21}/(A_{21} + Q_{21})$ accounts for the fluorescence signal losses due to non-radiating de-excitation. In particular, it is possible to follow the same assumption reported by Löhle and Auweter-Kurtz (2007) by considering the non-radiating processes summed up in the quenching rate. The fluorescence lifetime τ can be related to the fluorescence quantum yield as given by the eq. 2.

$$\frac{A_{21}}{A_{21} + Q_{21}} = A_{21} \tau \quad (2)$$

The Einstein coefficient of the spontaneous emission A_{21} is taken from literature, and it is equal to $2.89 \times 10^7 \text{ s}^{-1}$ (Niemi et al. 2001, Niemi et al. 2005) for the atomic oxygen and $2.45 \times 10^7 \text{ s}^{-1}$ for the xenon ($6p'[3/2]_2$) (Niemi et al. 2005).

The eq. 1 for unsaturated TALIF is applicable to both xenon and atomic oxygen taking the same experimental setup; the resulting expression of the oxygen number density n_o is given by eq. 3.

$$n_o = \frac{S_o}{S_{Xe}} \frac{E_{Xe}^2}{E_o^2} \frac{\eta_{Xe}}{\eta_o} \frac{A_{21Xe} \tau_{Xe}}{A_{21O} \tau_o} \frac{\sigma_{\omega,Xe}^{(2)}}{\sigma_{\omega,O}^{(2)}} \frac{g(\Delta\omega_{Xe})}{g(\Delta\omega_o)} n_{Xe} \quad (3)$$

The detection parameter D changes in terms of transmission coefficient of the spectral bandwidth filter and the quantum efficiency of the detector. These contributions are summarized in η for each species. The ratio of the cross sections $\sigma_{\omega,Xe}^{(2)}/\sigma_{\omega,O}^{(2)}$ calculated by Niemi et al. (2005) is equal to ~ 1.9 with an estimated uncertainty of 20%. The ratio of the linewidths $g(\Delta\omega_{Xe})/g(\Delta\omega_o)$ takes into account the different spectral response of the laser system in correspondence of the excitation wavelength (Niemi et al. 2001). In this work, this ratio has been included by integrating the fluorescence signal over the resonance as suggested by Goehlich et al. (1998).

Several technical solutions have been applied to implement TALIF experimental setup on arcjet and plasma facilities (Bamford et al. 1995, Del Vecchio et al. 2000, Takayanagi et al. 2009 and Marynowski et al. 2014). Bamford et al. 1995 implemented a sensor based on LIF to characterize the freestream of the arcjet flow at the 20-MW NASA Ames aerodynamic heating facility. Among others, they measured the number density of the atomic oxygen using a controlled source of atomic oxygen as reference. Subsequently, they estimated the number density in the freestream. Del Vecchio et al. 2000 used doubled laser light produced by a dye system pumped by a tunable excimer laser to probe atomic oxygen in the L2K facility. The fluorescence signal was captured by an Intensified CCD, pointed along the freestream. Even though, an estimation of absolute atomic concentration was not performed, they evaluated the temperature by analyzing the fine structure of the atomic oxygen from its Boltzmann plot. Takayanagi et al. 2009 obtained atomic oxygen concentration by using xenon as reference gas from TALIF measurements at the 750kW JAXA arcjet wind tunnel. The laser beam was guided into the test chamber forming a transverse path with respect to the axis of the arcjet. Spatial resolved measurements were performed by using an Intensified CCD camera to image the fluorescence signal. They carried out the spatial distribution of the number density of the atomic oxygen along the streamwise direction in presence of a blunt body. The parametric study conducted by varying the flow conditions reveals a direct dependency of the concentration of the atomic oxygen with respect to the mass flow rate. Similar calibration procedure was applied by Marynowski et al. 2014 in order to measure the number density of the atomic oxygen. Since the emission profile of the xenon is the convolution of the Lorentzian (in their experimental setup dominated by the laser) and Gaussian parts (due to the kinetic temperature of the probed species), they analyzed the line broadening of the emission profile of the atomic oxygen to calculate the translational temperature in the freestream. They found out that the number density deviates from the equilibrium value more than one order of magnitude, thus, concluding that the flow was not in local chemical equilibrium.

In this work, the atomic oxygen concentration of high enthalpy flows has been measured using TALIF technique. In particular, most interest is addressed to measure the absolute atomic oxygen concentration in the freestream and inside the shock layer, which is formed when the hypersonic flow field interacts with a blunt body. In the following, the description of the experimental setup, the technical solutions of the application of the TALIF in the arc heated facility L2K and the evaluation of the atomic oxygen concentration are outlined.

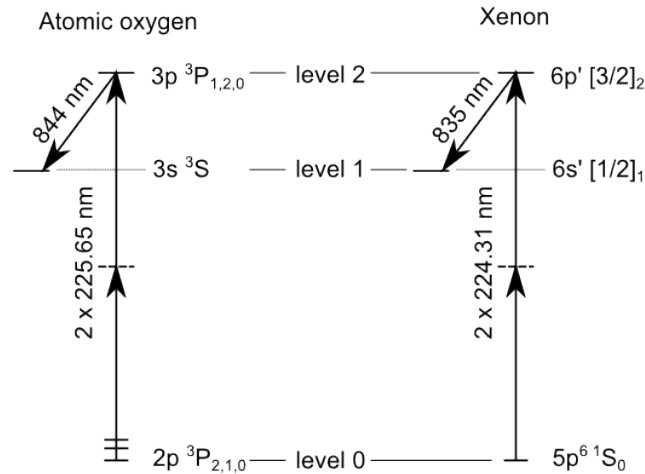


Fig. 1 Two-photon excitation schemes of the atomic oxygen (left) and xenon (right).

2. Experimental apparatus

2.1 L2K facility

The experiments have been conducted in the L2K facility at German aerospace research centre DLR in Cologne, Germany. The L2K facility is used for testing thermal protection materials under high aero-thermodynamic loads (Gülhan 1997).

L2K is an arc-heated jet facility equipped with a conventional Huels type arc heater with a maximum operative power of 1 MW; it is supplied with atmospheric air, as working gas, delivered by 10^3 m³ storage tank. For the present test campaign, an arc current of 600 A is set on the arc heater with a mass flow rate of 36 g/s and a stagnation pressure of 10^5 Pa. The temperature and the total enthalpy in the supply reservoir are estimated starting from the measured settling chamber pressure and the total mass flow rate and, then, by applying the equilibrium flow solution from the reservoir to the throat. The averaged total enthalpy delivered to the gases is equal to 8.4 MJ/kg and the temperature is assumed equal to 4218 K. The test conditions are summarized in Table 1. The high-enthalpy flow passes through a conical nozzle with longitudinal length of 400 mm and the expansion is achieved through a throat and an exit diameter equal to 29 mm and 200 mm, respectively. The test chamber has a cylindrical shape with a diameter of 2.6 m and a length of 2 m transversal to the flow direction. For a more detailed description of the L2K facility the reader is referred to Gülhan (1997).

In order to study the thermo-chemical effects concerning the interaction of a blunt body into a hypersonic flow, water-cooled flat faced cylindrical model with a diameter of 50 mm and with a rounded corner of 4 mm of radius is used. It is mounted on a holder with the axis aligned along the centerline of the nozzle. For the present experimental campaign, the model is placed at 160 mm downstream the nozzle exit.

L2K operating conditions at 1MW/m²		
Air		
mass flow rate	[g/s]	36
reservoir pressure	[Pa]	10 ⁵
reservoir temperature	[K]	4218
reservoir density	[kg/m ³]	0.0702
total enthalpy	[MJ/kg]	8.4

Table 1 Test operating conditions.

2.2 Optical setup

The main components of the optical setup are a tunable laser composed of three unities in cascade and a detection system. The first unit is Nd:YAG laser with an output beam set at 355 nm, the pulse duration is ~ 10 ns with a repetition rate of 10 Hz. The light from the Nd:YAG laser is used to pump a dye laser; in cascade for frequency doubling a beta barium borate BBO crystal produces an output laser beam with a maximum energy of ~ 500 μ J per pulse with a measured linewidth of 2.3 ± 0.05 pm. The final wavelength ranges in the ultraviolet (UV) radiation between 224.000 nm and 224.020 nm for the xenon investigation and 225.340 nm and 225.360 nm for the atomic oxygen investigation with a step width of ~ 0.5 pm. The energy of the UV radiation is varied by means of a variable attenuator (VA), which is installed through the optical path at the laser exit. An isometric view of the experimental setup is shown in Fig. 2. An ultrafast photodiode (PD) monitors the amount of the laser energy during its time evolution and it allows for time resolved measurements of the reference signal for the normalization (see eq. 3). A periscopic lens system composed of three dichroic mirrors (MDs) directs the laser beam into the L2K test chamber through an optical window. A positive focal lens is installed in the test chamber focalizing the laser beam at the measurement region located at ~ 155 mm downstream from the nozzle exit along the centerline. The final spatial resolution is equal to ~ 1 mm. The loss of the laser energy through the optical path has been evaluated by relating the energy at the laser exit for the levels 300, 400 and 500 μ J with that measured at the measurement region 100, 140 and 180 μ J, respectively. The averaged loss of energy is equal to 65% of that measured at the laser exit.

The fluorescence radiation is observed transverse with respect to the direction of the laser beam, i.e. $\sim 90^\circ$, and is collected by means of a detection system (DS). The DS is composed of two spherical Fused-Silica lenses, indicated in Fig. 2 as L1 and L2, with diameter of 1' and 2' and with -50 and 100 mm of focal length, respectively. By arranging in series L1 and L2 at the relative distance of ~ 54 mm, it is possible to collect the fluorescence radiation from the measurement

volume to the photocathode of a gated Hamamatsu H7680/-01 photomultiplier tube (PMT). An isometric view of the DS arrangement is sketched in the zoom of the Fig. 2. In order to select the light radiation coming from the plasma flow at the wavelengths of interest, an interference filter (IF) with a narrow bandwidth is installed through the optical detection path. As suggested by Niemi et al. (2005), a simplified experimental setup can be obtained by using the same IF for the atomic oxygen and xenon investigations without compromise the signal to noise ratio. The IF is centred at 840 nm with a full width at half-maximum equal to 10 nm; in particular, the transmission coefficients are equal to 30% and 37% for the wavelengths 844.9 and 834.9 nm, i.e., for the atomic oxygen and xenon (Niemi et al. 2005), respectively.

The fluorescence signal is acquired by a 300 MHz digital oscilloscope (Agilent Technologies InfiniiVision DSO6034A) with 4 channels; the data acquisition system integrates the oscilloscope by means of a home-built LabView software, which controls the acquisition and the storage of each fluorescence signal together with its related laser pulse. A signal generator (Agilent 33120), triggered by the pump laser, gates the PMT in order to capture the fluorescence signal (Fig. 2).

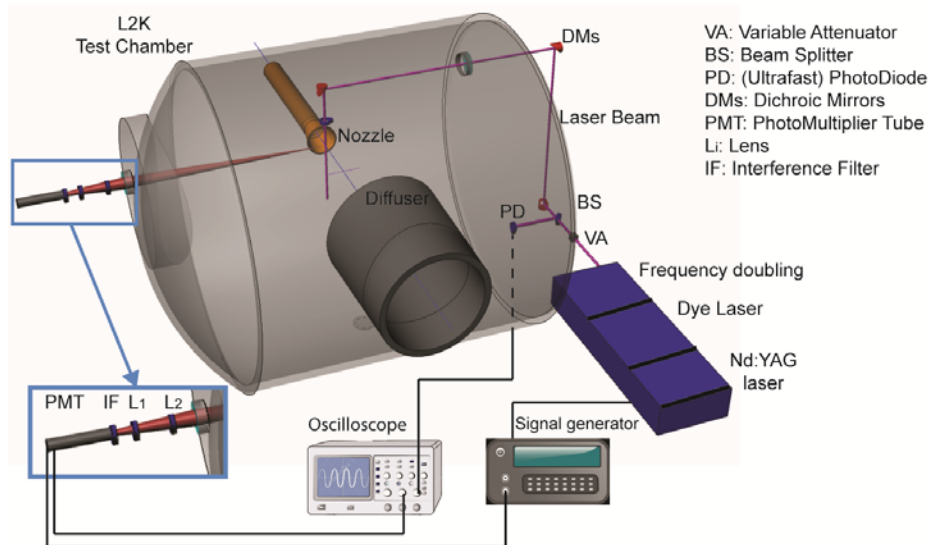


Fig. 2 L2K test chamber and TALIF experimental setup.

3. Results

The measurements of the xenon fluorescence are conducted in a cold reference gas cell (RGC) placed at the location of the probed volume, i.e., 5 mm upstream from the model surface. RGC is a hollow stainless-steel cross of perpendicular pipes and it is equipped with five optical accesses, which are aligned with respect to both the directions of the laser beam and the line of sight of the DS. After the vacuum procedure, the pressure reached in the RGC is $\sim 10^{-3}$ Pa, before its filling with the xenon gas. Because of the calibration procedure is based on a reference measurement with a noble gas at known concentration, the absolute pressure of the xenon at the room temperature equal to 19 °C is measured. A dataset of xenon fluorescence at four different

pressures, 139.0, 246.0, 344.0 and 698.0 Pa, has been acquired by scanning the wavelength of the laser (centered at 224.010 nm) and by varying the energy of the laser light in the range between 200 μJ and 400 μJ with step of 100 μJ .

In order to obtain better statistic convergence of the time resolved data, 10 uncorrelated samples are acquired for each investigated wavelength. An amount of 400 samples is acquired by ranging the wavelength in a 10-neighbourhood of 224.010 nm and of 225.350 nm for xenon and atomic oxygen species, respectively. The measurements have been conducted for xenon and atomic oxygen at different levels of energy of the laser light. In order to investigate the fluorescence signal quantitatively as concentration measurements, the linear dependency of the fluorescence signal with respect to the square of the laser energy has to be verified (Niemi et al. 2005). Fig. 3 shows the integrated signal of the fluorescence over time as a function of the laser energy. In Fig. 3a, the integrated fluorescence signal of the atomic oxygen exhibits a quadratic dependency with respect to the laser energy, the slopes of the linear fitting curves for the freestream and for the shock layer investigations are 2.01 ± 0.16 and 2.11 ± 0.20 , respectively. This discards the presence of saturation or ionization processes which can lead to a reduced fluorescence signal (Marynowski et al. 2014). However, in Fig. 3b the quadratic dependency is not satisfied for all investigated xenon $6p'[3/2]_2$ transitions at different pressure values. For xenon at 139 Pa, the linear fitting curve is characterized by a slope equal to 1.81 ± 0.09 , indicating a more pronounced tendency to the quadratic dependency than that at the other investigated pressures.

The fluorescence signal is averaged over 10 uncorrelated samples in order to identify the time evolution of the single fluorescence decay. Fig. 4 shows the averaged fluorescence signal of the xenon at 139 Pa and of the atomic oxygen detected in the freestream and into the shock layer, respectively. An exponential function is superimposed in order to evaluate the measured lifetime τ of the species. The fitting procedure is based on a Levenberg-Marquardt algorithm. In Fig. 4a, the fluorescence decay of the xenon exhibits a more pronounced scattered signal than that detected for the atomic oxygen. Even though the transmission coefficient of the IF filter in correspondence of the emission wavelength of the xenon is higher than that of the atomic oxygen, the maximum peak of the xenon signal is lower than that detected from the atomic oxygen species at the same experimental conditions. The fluorescence signal of the atomic oxygen increases in the shock layer (Fig. 4c) respect to the freestream investigation (Fig. 4b). Furthermore, it is reasonable to infer by analyzing the decay rate of the fluorescence signal that the amount of the atomic oxygen concentration is increased in the shock layer. Indeed, it is possible to take into account the de-excitation process due to the quenching by inspecting the lifetime τ of the atomic oxygen (eq. 2); τ is equal to 25.8 ns and 11.4 ns for the freestream and shock layer investigations, respectively.

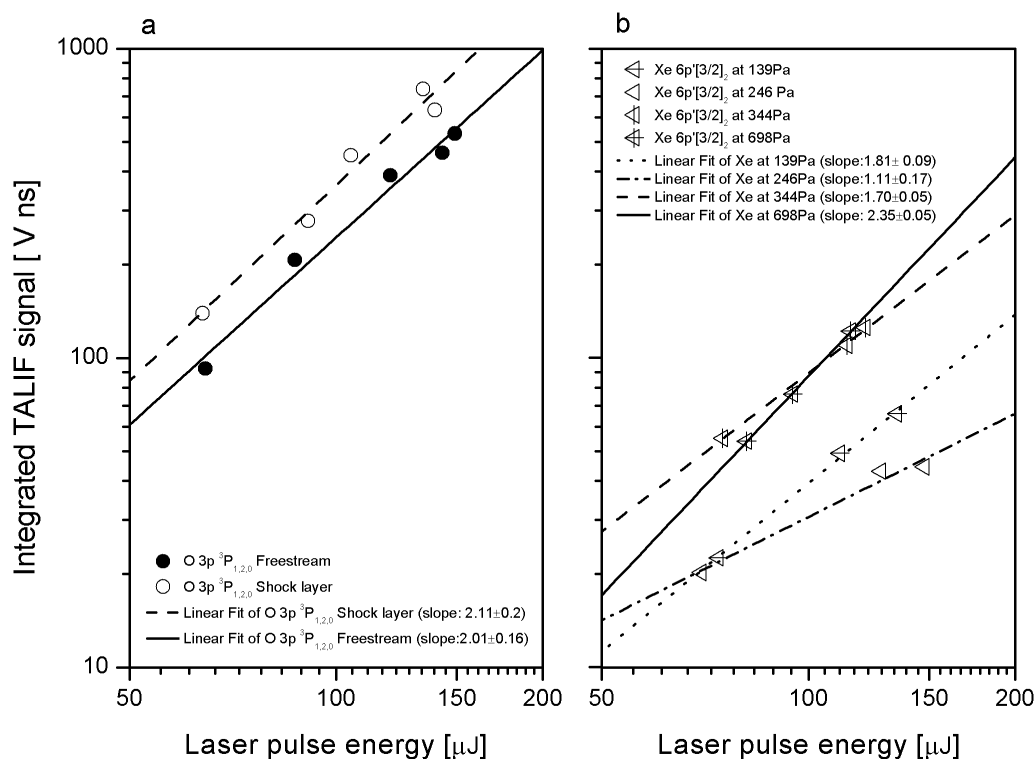


Fig. 3 Integrated fluorescence signal over time with respect to the square of the laser intensity and linear fitting for atomic oxygen (a) and for xenon (b).

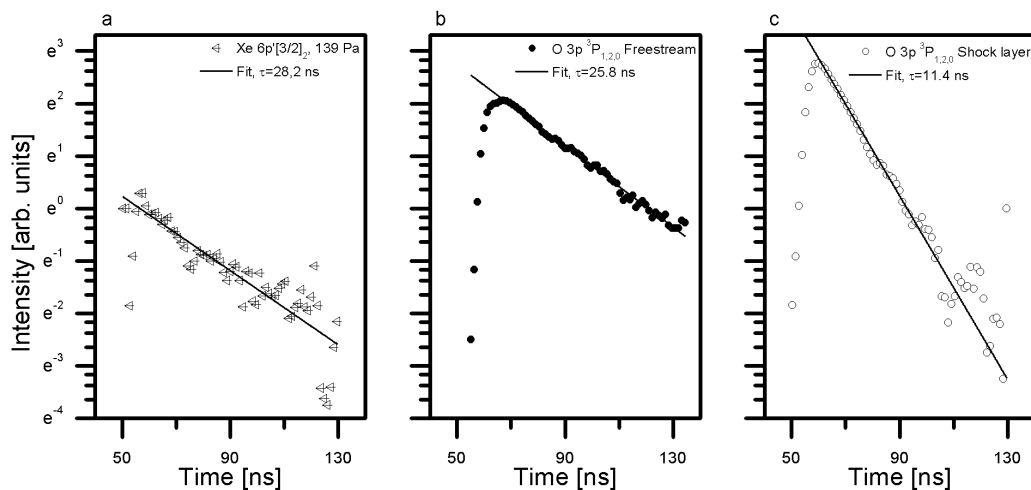


Fig. 4 Averaged fluorescence signal of the xenon (a) at the pressure of 139 Pa and atomic oxygen in the freestream (b) and in the shock layer (c); the exponential fitting curve is superimposed.

With this approach, the lifetime of the xenon at each pressure is calculated for different laser energies. In Fig. 5, the inverse lifetime with respect to the pressure (Stern-Volmer plot) is shown and it is compared to the results extracted from Niemi et al. (2005). It should be noted that the fitting curve with linear regression calculated from the inverse lifetime for the laser energy ~ 300 μJ is characterized by an intercept equal to ~ 0.024 ns^{-1} in agreement with Niemi et al. (2005). At

laser energy of $\sim 400 \mu\text{J}$, the fitting curve is translated in vertical direction and it is characterized by an intercept equal to $\sim 0.027 \text{ ns}^{-1}$ in agreement with that found by Eichhorn et al. (2011). These findings indicate that the experimental setup allows the calibration for quantitative TALIF measurements.

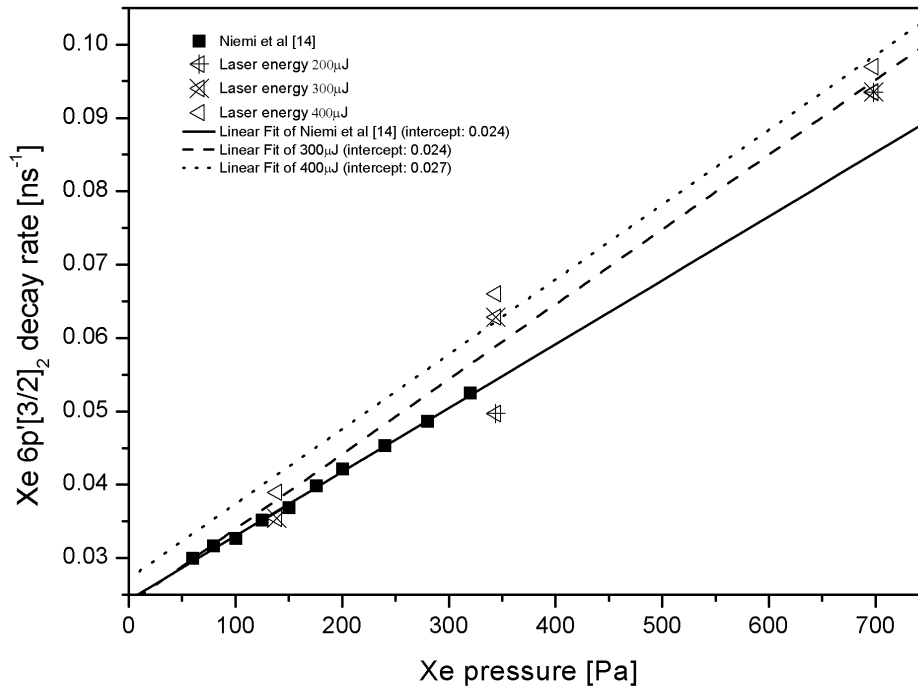


Fig. 5 Inverse lifetime with respect to pressure calculated from the xenon $6p' [3/2]_2$ TALIF measurements for different laser energies (left point triangle) and data extracted from Niemi et al. (2005) (square), linear fitting curves are superimposed.

Following the approach presented by Marynowski et al. (2014), it is possible to characterize the experimental setup in terms of instrumental line broadening from the calibration with xenon if the spectral profile of the laser is dominated by a Lorentzian shape. For the present experimental setup, this assumption can be applied. Fig. 6 shows the absorption line profile of the xenon at cold gas condition, i.e. room temperature 292K, and pressure 139 Pa. The line fitting is based on an approximated Voigt function (Pseudo-Voigt), based on the convolution of a Gaussian function with a Lorentzian function (Whiting 1968). The Gaussian and Lorentzian parts contribute to the Voigt function with the broadening due to the kinetic temperature $\Delta\lambda_{G,Xe}$ and with the instrumental broadening $\Delta\lambda_{instr}$, respectively. In the fitting procedure, the doppler part $\Delta\lambda_{G,Xe}$ is locked at the constant value of 0.12 pm. The resulting $\Delta\lambda_{instr}$ value is 3.1 pm, near the linewidth of the laser light for the present experimental setup. However, it is worth to note that the instrumental broadening is one order of magnitude higher than the Doppler one. Thus, the

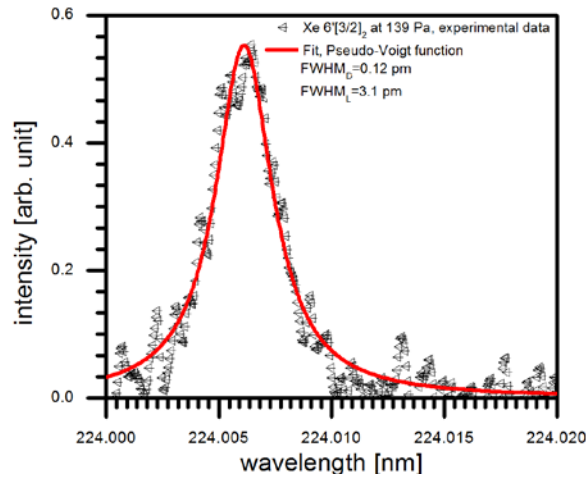


Fig. 6 Absorption profile of xenon ($6p' [3/2]_2$) at cold gas cell condition 139Pa, Pseudo-Voigt fitting (continuous line) is superimposed.

spectral resolution of the laser system does not allow for the evaluation of the translational temperature of the atomic oxygen at the investigated thermodynamic conditions. On the other hand, a qualitative inspection of Fig. 7 highlights that the contribution of the doppler broadening in the absorption profile increases from the value 1.3 pm to 2.3 pm. As expected, the temperature increases in the shock layer respect to the freestream condition.

The integral of the absorption profiles, i.e. the fluorescence signal of the xenon and atomic oxygen, enables the calculation of the absolute number density of the atomic oxygen by applying the eq. 3. For the operating condition of the L2K facility (Table 1), the atomic number density is measured in the freestream and into the shock layer at 300 μ J of laser energy and xenon pressure 139 Pa as reference. It is equal to $\sim 3.33 \times 10^{23} \text{ m}^{-3}$ in the freestream and $\sim 15.6 \times 10^{23} \text{ m}^{-3}$ into the shock layer. The ratio of the standard deviation over the average is equal to $\sim 4\%$, within the overall uncertainty, i.e. $\sim 20\%$ relative to the estimation of the ratio of the cross sections, $\sigma_{\omega, \text{Xe}}^{(2)} / \sigma_{\omega, 0}^{(2)}$ (Niemi et al. 2005). Thus, the atomic oxygen concentration into the shock layer is about ~ 4.7 times greater than that measured in the freestream.

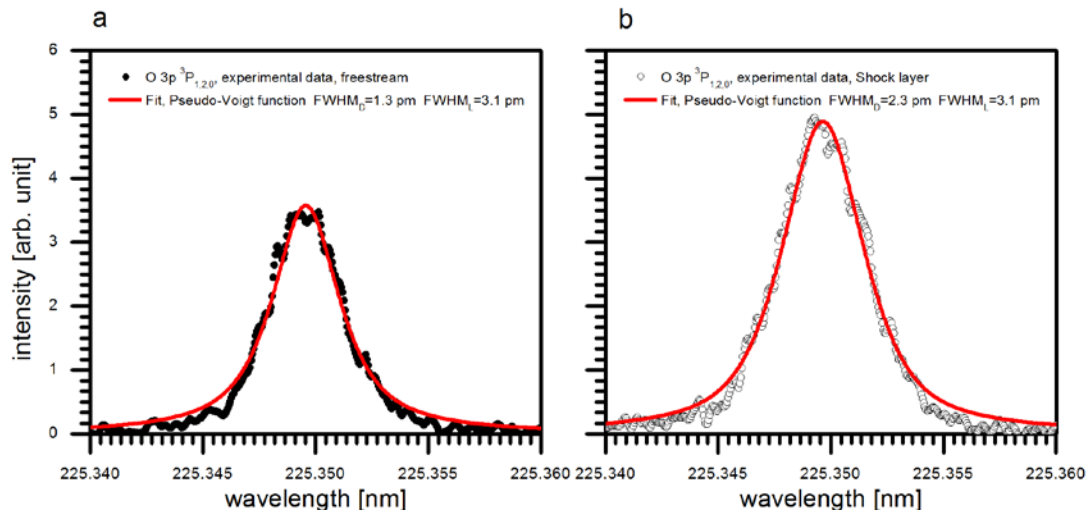


Fig. 7 Absorption profile of the atomic oxygen $O\ 3p\ ^3P_{1,2,0}$, Pseudo-Voigt fitting curve (continuous line) is superimposed.

4. Conclusions

This work presents absolute atomic oxygen concentration measurements performed at L2K facility by using TALIF experimental method. TALIF experimental setup is implemented at the test chamber of the L2K facility. This setup allows for the investigation of the atomic oxygen concentration arising in high enthalpy flows with air as working gas. For the test campaign, arc current is set at 600 A with a mass flow rate of 36 g/s and a stagnation pressure of 10^5 Pa. The mass averaged total enthalpy is about ~ 8.4 MJ/kg and the temperature is assumed to be equal to 4218 K.

In order to provide quantitative measurements of the atomic oxygen concentration, TALIF calibration procedure is performed by using xenon transition $6p' [3/2]_2$. The estimation of the atomic oxygen concentration is based on the analysis of the measured line profiles of both the investigated species. The measured value in the freestream and into the shock layer is equal to $\sim 3.33 \times 10^{23} \text{ m}^{-3}$ and $\sim 15.6 \times 10^{23} \text{ m}^{-3}$, respectively. The atomic oxygen dissociation increases into the shock layer reaching an increment of about ~ 4.7 times greater than the concentration estimated in the freestream.

Acknowledgements

This research has been conducted as part of the ABLAMOD project funded by the European Community's Seventh Framework Program.

References

- Anderson J D (2000). Hypersonic and high temperature gas dynamics. AIAA.
- Bamford DJ, O'Keefe A, Babikian D S, Stewart DA, and Strawa AW (1995) Characterization of arcjet flows using laser-induced fluorescence. *Journal of thermophysics and heat transfer*, 9(1):26-33.
- Candler G, Nompelis I, Druguet MC, Holden MS, Wadhams TP, Boyd ID and Wang L (2002) CFD Validation for Hypersonic Flight - Hypersonic Double-Cone Flow Simulations. 40th AIAA Aerospace Sciences Meeting and Exhibit, January 14-17.
- Eichhorn C, Löhle S, Fasoulas S, Leiter H and Auweter-Kurtz M (2011) Laser Induced Fluorescence Spectroscopy on Neutral Xenon: Two-Photon Cross Sections and Measurements in an Ion Thruster Plume. In 42nd AIAA Plasmadynamics and Lasers Conference, Honolulu, AIAA Paper (Vol. 3460).
- Goehlich A, Kawetzki T and Döbele HF (1998) On absolute calibration with xenon of laser diagnostic methods based on two-photon absorption. *The Journal of chemical physics*, 108(22): 9362-9370.
- Gülhan A (1997) Arc Heated Facility LBK as a Tool to Study High Temperature Phenomena at Re-entry Conditions.
- Löhle S and Auweter-Kurtz M (2007) Laser-induced fluorescence measurements of atomic oxygen using two calibration methods. *Journal of thermophysics and heat transfer*, 21(3): 623-629.
- Marynowski T, Löhle S and Fasoulas S (2014) Two-Photon Absorption Laser-Induced Fluorescence Investigation of CO₂ Plasmas for Mars Entry. *Journal of Thermophysics and Heat Transfer*, 28(3): 394-400.
- Niemi K, Schulz-Von Der Gathen V and Döbele HF (2001) Absolute calibration of atomic density measurements by laser-induced fluorescence spectroscopy with two-photon excitation. *Journal of Physics D: Applied Physics*, 34(15): 2330.
- Niemi K, Schulz-Von Der Gathen V and Döbele HF (2005) Absolute atomic oxygen density measurements by two-photon absorption laser-induced fluorescence spectroscopy in an RF-excited atmospheric pressure plasma jet. *Plasma Sources Science and Technology*, 14(2): 375.
- Sharma SP and Park C (1990) Survey of simulation and diagnostic techniques for hypersonic nonequilibrium flows. *Journal of thermophysics and heat transfer*, 4(2): 129-142.
- Sharma SP, Park CS, Scot CD, Arepalli S and Taunk J (1996) Arcjet flow characterization. AIAA Paper, 96-0612.
- Takayanagi H, Mizuno M, Fujii K, Suzuki T and Fujita K (2009) Arc Heated Wind Tunnel Flow Diagnostics using Laser-Induced Fluorescence of Atomic Species. *laser*, 500, 2.
- Tropea C, Yarin AL and Foss JF (2007) Springer Handbook of Experimental Fluid Mechanics. Springer Science and Business Media.
- Del Vecchio A, Palumbo G, Koch U and Guelhan A (2000) Temperature Measurements by Laser-Induced Fluorescence Spectroscopy in Nonequilibrium High-Enthalpy Flow. *Journal of Thermophysics and Heat Transfer* 14(2): 216-24.
- Whiting EE (1968) An Empirical Approximation to the Voigt Profile. *Journal of Quantitative Spectroscopy and Radiative Transfer* 8(6): 1379-84.

